Wnt/β-catenin signaling requires interaction of the Dishevelled DEP domain and C terminus with a discontinuous motif in Frizzled

Daniele V. F. Tauriello[a,1,2], Ingrid Jordens[a,1], Katharina Kirchner[b,3], Jerry W. Slootstra[c,3], Tom Kruitwagen[a], Britta A. M. Bouwman[a], Maria Noutsou[a], Stefan G. D. Rüdiger[d], Klaus Schwamborn[c], Alexandra Schambony[b], and Madelon M. Maurice[a,4]

[a]Department of Cell Biology, University Medical Center Utrecht, 3584 CX Utrecht, The Netherlands; [b]Developmental Biology Unit, Department of Biology and Developmental Biology, Friedrich-Alexander University Erlangen-Nuremberg, 91058 Erlangen, Germany; [c]Pepscan Therapeutics BV, 8243 RC Lelystad, The Netherlands; and [d]Cellular Protein Chemistry, Bijvoet Center for Biomolecular Research, Utrecht University, Utrecht, 3584 CH Utrecht, The Netherlands

Wnt binding to members of the seven-span transmembrane Frizzled (Fz) receptor family controls essential cell fate decisions and tissue polarity during development and in adulthood. The Fz-mediated membrane recruitment of the cytoplasmic effector Dishevelled (Dvl) is a critical step in Wnt/β-catenin signaling initiation, but how Fz and Dvl act together to drive downstream signaling events remains largely undefined. Here, we use an Fz peptide-based microarray to uncover a mechanistically important role of the bipartite Dvl DEP domain and C terminal region (DEP-C) in binding a three-segmented discontinuous motif in Fz. We show that cooperative use of two conserved motifs in the third intracellular loop and the classic C-terminal motif of Fz is required for DEP-C binding and Wnt-induced β-catenin activation in cultured cells and Xenopus embryos. Within the complex, the Dvl DEP domain mainly binds the Fz C-terminal tail, whereas a short region at the Dvl C-terminal end is required to bind the Fz third loop and stabilize the Fz-Dvl interaction. We conclude that Dvl DEP-C binding to Fz is a key event in Wnt-mediated signaling relay to β-catenin. The discontinuous nature of the Fz-Dvl interface may allow for precise regulation of the interaction in the control of Wnt-dependent cellular responses.

peptide microarray | protein-protein interaction | Wingless signaling

The Wnt family of secreted glycolipoproteins controls key cellular processes in embryonic development and stem cell maintenance in multicellular animals. Deregulation of Wnt pathway components is associated with various human diseases, most notably cancer (1–3). Depending on the cellular context, Wnts can induce distinct intracellular signaling cascades of which the Wnt/β-catenin and planar cell polarity (PCP) pathways are best described (4–6). Both pathways are initiated by Wnt-mediated activation of members of the Frizzled (Fz) receptor family, followed by the recruitment of the cytoplasmic effector protein Dishevelled (Dvl) to the plasma membrane (PM) (7–9). Downstream signaling cascades are remarkably divergent, however, leading to the activation of β-catenin–mediated gene transcription in the control of cell fate decisions or to small GTPase-mediated cytoskeletal remodelling in the planar polarization of epithelia (5, 10). How the common Fz-Dvl signaling unit distinguishes among different Wnt pathways remains obscure. Insight into the molecular basis by which Fz–Dvl complexes are formed at the PM is essential to understand how cell fate choices and morphogenesis are orchestrated.

The Fz family of Wnt receptors comprises G protein-coupled receptor (GPCR)–like transmembrane proteins (7, 11–13). Fz carries an extracellular N-terminal cysteine-rich domain, which mediates Wnt binding, followed by a seven-span transmembrane signaling moiety (Fig. 1A). The cytoplasmic C-terminal tail of Fz contains a conserved motif (KTxxxW) that is essential for signaling and for membrane relocalization of Dvl (9, 14, 15). Microinjection of peptides comprising this motif interferes with Wnt/β-catenin signaling in Xenopus embryos, further supporting the functional importance of the Fz C-terminal tail. Mutagenesis studies have revealed, however, that other Fz regions, including the intracellular loops, contribute to Wnt signaling by unknown mechanisms (14, 16–18). Indeed, overexpressed Drosophila Fz2 lacking its C-terminal tail still synergizes with Wnt in Dvl-dependent signaling (19).

Dvl is a cytoplasmic scaffold protein of which three homologs exist in vertebrates (Dvl1, Dvl2, and Dvl3). Dvl carries three structurally conserved domains that are functional in Wnt-induced signaling responses. The N-terminal DIX domain mediates Dvl self-association, leading to the formation of multimerized receptor complexes at the membrane, which are proposed to drive signaling positively by providing a high local concentration of binding sites for Wnt signaling proteins (20–22).

The PDZ domain, located in the central region of Dvl, was shown to bind an Fz7-derived peptide containing the conserved KTxxxW motif in vitro (23). The relative low affinity of this interaction suggested the need for additional molecular interactions in the formation of a stable Fz–Dvl complex in vivo in cells. Moreover, the binding cleft of Dvl PDZ appears highly flexible and accommodates binding of a diverse set of peptide ligands in vitro as well as numerous Dvl PDZ binding partners in cells (24–26). How these interactors compete for Dvl PDZ domain binding and how specificity is achieved during Wnt signaling remain unresolved.

The conserved DEP domain, located in the C-terminal half of Dvl, is critical for membrane recruitment of Dvl during Wnt-mediated signaling (8, 27–30). Direct binding of a polybasic stretch in the DEP domain to negatively charged lipids was recently shown to contribute to formation of the Fz–Dvl complex at the PM (30). In addition, the Dvl2 DEP domain, aided by a YHEL motif in the Dvl C terminus, interacts with μ2-adaptin, a subunit of the AP-2 clathrin adaptor complex, to facilitate clathrin-mediated endocytosis of Fz4 and Dvl2 on Wnt activation

A

mFz5 — CRD

Intracellular loop 3
VSLFRIRSVIKQGGTKTDKLEKLMIRIGIF
VSLFRIRSV
SLFRIRSVI
LFRIRSVIK
......
22x 9-mers

C-terminal tail (30 AA)
WIWSGKTLESWRRFTSRAAASSGHKSGG
WIWSGKTLE
IWSGKTLES
WSGKTLESW
......
22x 9-mers

HIS-mDvl1 ΔDIX
Peptide library

22 x 22
G ☐ G ■ G
484 Linear

484 Scaffolded

B

ΔDIX — Ranked peptides

Rank #	Peptide #	Peptide Sequence	BI: AU	Normalized
1	158	GSLFRIRSVIGLESWRRFTSG	1179	2.96
2	156	GKLMIRIGIFGTLESWRRFTSG	1174	2.95
3	157	GVSLFRIRSVGLESWRRFTSG	1147	2.88
4	136	GSLFRIRSVIGTLESWRRFTSG	1118	2.81
5	154	GLEKLMIRIGGTLESWRRFTSG	1092	2.74
6	178	GKLMIRIGIFGLESWRRFTSG	1080	2.71
7	153	GKLEKLMIRIGTLESWRRFTSG	1066	2.68
8	155	GEKLMIRIGIGTLESWRRFTSG	1066	2.68
9	177	GEKLMIRIGIGLESWRRFTSG	1013	2.54
10	135	GVSLFRIRSVGTLESWRRFTG	993	2.49
...	...	...	...	...

C

Frequency in the top 5% — Motif III / Other

(bar chart over peptides: VSLFRIRSV, SLFRIRSV, LFRIRSVIK, FRIRSVIKQ, RIRSVIKQGG, IRSVIKQGGT, RSVIKQGGTK, SVIKQGGTKT, VIKQGGTKTD, IKQGGTKTDK, KQGGTKTDKL, QGGTKTDKLE, GGTKTDKLEK, GTKTDKLEKL, TKTDKLEKLM, KTDKLEKLMI, TDKLEKLMIR, DKLEKLMIRI, KLEKLMIRIG, LEKLMIRIGI, EKLMIRIGI, KLMIRIGIF)

D

iLoop 3 — Motif I, Motif II ... Tail — Motif III, Classical KTxxxW motif

E

	Motif I		Motif II
Fz1	VSLFRIRT	IMKHD--GTKTE	KLEKLMVRIGVF
Fz7	VSLFRIRT	IMKHD--GTKTE	KLEKLMVRIGVF
Fz2	VSLFRIRT	IMKHD--GTKTE	KLERLMVRIGVF
DFz	ISLFRIRT	VMKTD--GKRTD	KLERLMLRIGFF
Fz5	VSLFRIRS	VIKQ--GGTKTD	KLEKLMIRIGIF
Fz8	VSLFRIRS	VIKQQGGPTKTH	KLEKLMIRLGLF
Fz10	VALFHIRR	VMKTG--GENTD	KLEKLMVRIGVF
Fz4	VALFKIRS	NLQKD--GTKTD	KLERLMVKIGVF
Fz9	VALFHIRK	IMKTG--GTNTE	KLEKLMVKIGVF
Fz3	ISLNRVRI	EIPLE--KENQD	KLVKFMIRIGVF
Fz6	ISLNHVRQ	VIQHD--GRNQE	KLKKFMIRIGVF

Fig. 1. Identification of a discontinuous Dvl1 binding site in Fz5. (A) (Left) Schematic depiction of the topology of Fz proteins. iLoop3 and the C-terminal tail are boxed. (Right) Design of the Fz5 iLoop3-tail peptide library, based on 30 amino acids from mouse Fz5 iLoop3 (white) and 30 membrane-proximal amino acids from the Fz5 tail (black). Linear 9-mer peptides (22 each) were combined in *cis,* flanked and separated by Gly or Cys residues. CLIPS technology was used on Cys-based combinations, yielding bicyclical peptides; Gly-linked peptides were left linear. The combinatory peptides were immobilized in 455-well plates. Binding of recombinant His-tagged Dvl1-ΔDIX (G86–M695) was determined by an ELISA-based assay. (B) Binding signals were ranked by binding intensity (BI), and the 10 best binding peptides are depicted with their absolute score and normalized BI (relative to the screen average). AU, Arbitrary Units. (C) Frequency analysis of the top 5% (48 best binding peptides) reveals a strong preference for binding two motifs in iLoop3 (motifs I and II; pink and green) and one in the C terminus (motif III; blue). Motif III overlaps with the classic PDZ binding motif. Depicted are the frequencies of iLoop3 peptides in the top 5%, whether combined to motif III (blue) or not (white; other). (D) Diagram of the three Dvl1 binding motifs in the mFz5 iLoop3 and C-terminal tail. (E) Alignment of regions encompassing motifs I and II of mouse Fz family members and *Drosophila* Fz (DFz). Motifs I and II are highly conserved among most Fzs.

(31, 32). Both of these activities of the DEP domain are mainly linked to PCP signaling, however, leaving the role of the DEP domain in β-catenin–dependent signaling unexplained (29, 33–36). Moreover, a number of point mutants in the DEP domain were uncovered that, based on their location in the structure, do not participate in lipid or AP-2 binding yet prevent the translocation of Dvl to the PM (27–29).

Progress in the understanding of how Fz and Dvl function together during Wnt signaling is hampered by the general lack of biochemical evidence for their interaction, partly attributable to the hydrophobic nature of the Fz protein. Here, we use a peptide scanning method to address the molecular basis of complex formation between Fz and Dvl. We show that the Dvl DEP domain and C-terminal region (DEP-C) mediates direct binding to a three-segmented discontinuous motif in Fz, composed of the third intracellular loop (iLoop3) and C-terminal tail. The individual Dvl binding sequences in the cytosolic interface of Fz cooperate to form stable Fz–Dvl complexes at the PM and initiate Wnt/β-catenin signaling. With these findings, we assign a previously unknown molecular activity to the Dvl DEP domain, identify a functional role of the Dvl C-terminal region, and place the DEP-C domain central to Wnt/β-catenin signaling initiation.

Results

Identification of a Discontinuous Dvl Binding Surface in the Fz Receptor.

To gain insight into the binding mode between mouse Fz5 and Dvl1, we combined high-throughput PEPSCAN microarray technology (Pepscan Therapeutics BV) with spatially defined peptide conformations [chemically linked peptides on scaffolds (CLIPS) technology (37)] to mimic the cytoplasmic interface of Fz5 and facilitate the discovery of complex molecular recognition modes between Fz and Dvl. We generated a combinatorial peptide library comprising 9-mer peptides of the Fz5 iLoop3 (V424–F453) in *cis*-combination with 9-mer peptides from the proximal region of the C-terminal tail of Fz5 (W520–G550) (Fig. 1A). Peptides were flanked by either glycines or cysteines. Glycine-flanked peptides were left in a linear conformation, whereas cysteine-flanked peptides were imposed on a trivalent chemical scaffold to mimic a looped conformation (37). To allow for specificity of cysteine-based chemical modifications, the three native cysteines in the distal part of the Fz5 tail were changed to alanines in the 9-mer peptides. The library, containing 968 combinatorial iLoop3-tail peptides in total, was immobilized on 455-well plates (Fig. 1A).

Tauriello et al.

We purified His-tagged, recombinant mouse Dvl1-ΔDIX (G86–M695) protein and investigated its binding to the Fz5 peptide library through detection with peroxidase-conjugated anti–His-tag antibodies. The resulting values were ranked according to binding signal, and the top 5% of best binding peptides were analyzed for the presence of prevalent Dvl binding motifs (Fig. 1 B and C). Clearly, Dvl1-ΔDIX displays a strong preference for binding three linear motifs in Fz5 (Fig. 1D). In the Fz5 C-terminal tail, Dvl1-ΔDIX binds a sequence that overlaps with the known PDZ binding motif (Fig. 1D, motif III). In Fz5 iLoop3, Dvl1-ΔDIX binds two sequences that flank predicted TM regions 5 and 6 (Fig. 1D, motifs I and II). Both Dvl binding motifs in Fz5 iLoop3 are highly conserved among Fz family members, although loss of conservation of motif I is evident in Fz3 and Fz6 (Fig. 1E). Strikingly, Dvl1-ΔDIX strongly preferred binding to linear Fz5 peptides that combined either motif I or II with motif III (Fig. 1C). Scaffolded, bicyclical Fz5 peptides in looped conformation displayed an identical binding pattern, albeit with overall lower binding, suggesting that flexibility of the individual motifs accommodates optimal Dvl1 interaction. These results indicate that Dvl binds to both iLoop3 and the C-terminal tail of Fz in a cooperative manner.

Dvl Binding Motifs I and II in Fz5 iLoop3 Are Essential for Wnt/β-Catenin Signaling and Recruitment of Dvl in Human Cells. To address the importance of the Fz5 iLoop3 residues in signaling, we performed triple alanine-scanning mutagenesis of motifs I and II and compared expression and signaling of the resulting Fz5 variants in HEK293T cells. The majority of Fz5 mutants showed similar expression as WT Fz5, but alanine substitution of the residues flanking the sixth TM region (^{449}RIGIF^{453}) caused retention of Fz5 in the endoplasmic reticulum (ER), as indicated by the lack of glycosylated, mature Fz on immunoblotting as well as an ER-associated subcellular localization (Fig. 2B). We conclude that this TM proximal region is essential for Fz maturation or sorting, and thus precludes further investigation. All other Fz5 mutants were processed to the mature form and transported to the PM (Fig. 2B), allowing for analysis of their signaling propensity.

Overexpression of Fz5 in HEK293T cells strongly induced β-catenin-dependent transactivation of a luciferase reporter plasmid (TOPflash) on stimulation with Wnt3a-conditioned medium (Fig. 2A). Single alanine substitutions of key residues in the classic Dvl binding motif in the Fz5 C terminus significantly impaired signaling, as expected (9, 16) (Fig. 2C). To address the individual contribution of motifs I and II to Fz5-mediated signaling, we applied single alanine substitutions to pin down critical residues in these motifs. Mutation of individual residues in Fz5 motif I (I429A and R430A) or motif II (L443A and L446A) strongly reduced or completely abrogated signaling, respectively [Fig. 2 A (arrows) and C]. In contrast, mutation of the connecting
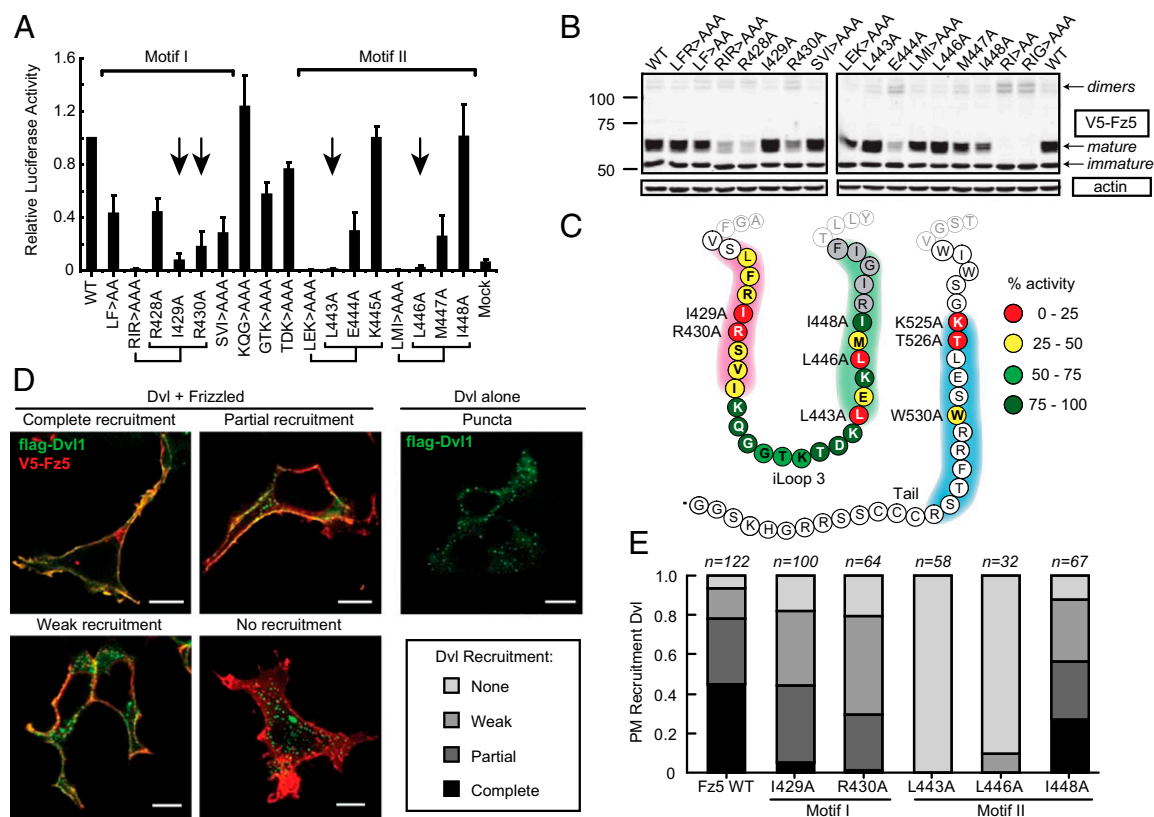
Fig. 2. iLoop3 motifs I and II in Fz are essential for Wnt/β-catenin signaling and PM recruitment of Dvl. (A) Alanine scan of iLoop3 residues within full-length Fz5. Fz5 mutants were tested in the TOPFlash luciferase reporter assay and compared with WT Fz5. HEK293T cells were transfected with either TOPFlash or FOPFlash firefly luciferase reporter, thymidine kinase-Renilla control plasmid, and the indicated mFz5 constructs or empty vector (Mock). Cells were treated overnight with Wnt3a-conditioned medium. Firefly/Renilla values of TOPFlash/FOPFlash are given as normalized averages from at least three individual experiments; error bars depict SDs. Critical single residues within motifs I and II for Fz function are indicated with arrows. (B) Immunoblot expression analysis of V5-Fz5 variants, transfected in HEK293T cells; actin loading controls are shown. Immature (ER) and fully glycosylated mature Fz as well as SDS-resistant Fz dimers are indicated. (C) Color-coded luciferase activity map of iLoop3 alanine-scanning data. Fz5 mutations that caused ER retention are indicated in gray. (D) Categories of Flag-Dvl1 recruitment to Fz5 mutants as analyzed by confocal immunofluorescence microscopy are shown. (Scale bars: 10 μm.) (E) Inactive Fz5 iLoop3 point mutants display impaired Flag-Dvl1 recruitment. Motif I mutants show an intermediate recruitment phenotype, and motif II mutations L443A and L446A fail to recruit Dvl1. WT and a control mutant (I448A) are also depicted. The number of counted cells per condition is indicated.

Tauriello et al.

sequence between motifs I and II did not interfere or just slightly interfered with signaling (Fig. 2A). Because mutation of single residues in motif I, motif II, or motif III abrogates Fz function in Wnt/β-catenin signaling, we propose that the three Dvl binding motifs comprise a discontinuous Dvl binding surface (Fig. 2C).

To investigate whether the Fz5 iLoop3 motifs I and II contribute to Dvl binding in cells, we studied PM recruitment of Dvl1 in HEK293T cells coexpressing WT or mutant Fz5. In contrast to WT Fz5, motif II mutants (L443A and L446A) failed to recruit coexpressed Flag-Dvl1; instead, Dvl localized to its characteristic cytoplasmic puncta (21). Fz5 motif I mutants (I429A and R430A) displayed an intermediate phenotype. The control Fz5 variant I448A, however, which signaled equally well as WT Fz5, displayed robust Dvl recruitment (Fig. 2 A and E). We conclude that, in addition to the classic C-terminal Fz motif, iLoop3 motif II is required for Dvl binding and signaling in the cellular context and that motif I significantly contributes to this binding mode.

Fz Discontinuous Binding Motif Is Required for Wnt/β-Catenin Signaling and Dvl Recruitment in Vivo. To address whether the signaling role of Fz5 motifs I and II is conserved across species, we generated a set of *Xenopus* Fz7 (XFz7) variants with mutations in critical iLoop3 residues equivalent to those of mFz5. WT XFz7 induces enhanced TOPFlash luciferase reporter activity in

HEK293T cells when stimulated with Wnt3a. Similar to our findings with mFz5, XFz7 motif I and motif II single mutants abrogated luciferase reporter activity, with the strongest effects of mutations in motif II (Fig. 3A).

To determine the functional relevance of the iLoop3 Dvl binding motifs further, we analyzed *Xenopus* embryo body axis duplication by ectopic Wnt/Fz-mediated β-catenin activation at the ventral side. We injected a subeffective dose of XWnt8 combined with each of the XFz7 variants to compare their ability to induce double axis formation. Expression of XFz7 motif I mutant I425A strongly reduced viability of the embryos and was precluded from further analysis. XFz7 motif II mutants L439A and L442A displayed a significant reduction in Wnt-induced double axis formation in comparison to WT XFz7 as well as control mutant V444A, suggesting impaired function in vivo (Fig. 3 B and C). XFz7 motif I mutant R426A displayed an intermediate phenotype (Fig. 3 B and C), in agreement with the partial activity observed in the TOPFlash assay (Fig. 3A). In addition, XDvl2 recruitment mediated by XFz7 motif I and II mutants expressed in animal cap explants was partially and strongly impaired, respectively (Fig. 3 D and E). We conclude that Fz iLoop3 motifs I and II are functionally conserved in Fzs across species and that Dvl2 follows similar binding requirements as Dvl1. Also, motif II is more important for Fz-Dvl binding and signaling.
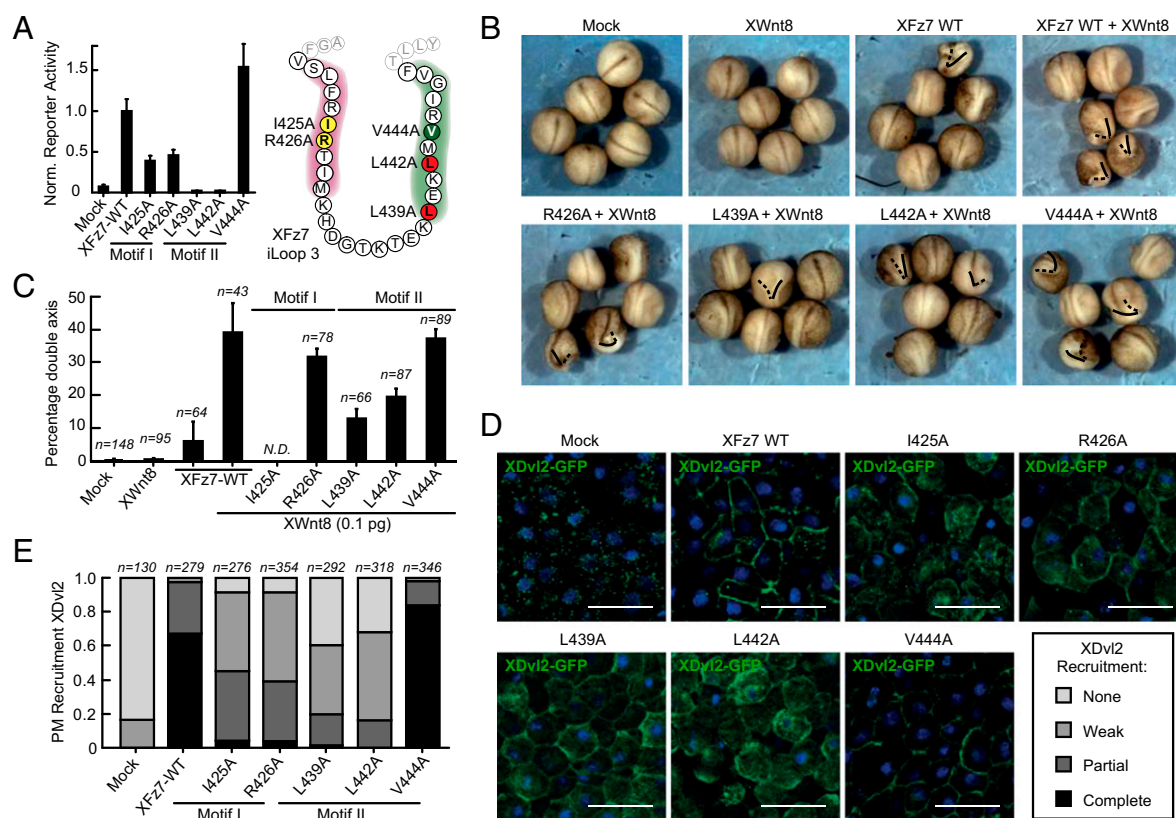
Fig. 3. XFz7 motifs I and II are essential for Wnt-mediated signaling and XDvl2 recruitment in *Xenopus* embryos. (A) XFz7 iLoop3 motif I and II mutants display decreased Wnt3a-induced signaling. Indicated motif I and II XFz7 mutants were tested in the TOPFlash luciferase reporter assay as in Fig. 2A. (Left) Shown are the average normalized values of three individual experiments; error bars indicate SDs. Mock, empty vector. (Right) Color-coded activity map of tested XFz7 iLoop3 residues (as in Fig. 2C). (B) XFz7 motif II mutants are defective in secondary axis formation in *Xenopus* embryos. Ventral injections of combined mRNAs encoding for XFz7 variants and XWnt8 were used to compare β-catenin–mediated secondary axis formation. The primary axis is indicated by straight lines, and (partial) secondary axes are indicated by dotted lines. (C) Quantification of the results presented in B. XFz7 I425A caused severe embryonic lethality and was not quantified. Shown are the average percentages of axis duplication of three independent experiments; error bars depict SEs. The number of counted embryos per condition is indicated. (D) Colocalization of XFz7 motif I and II mutants and XDvl2-GFP in *Xenopus* animal cap explants is impaired. (Scale bars: 100 μm.) (E) Quantification of the results in D (as in Fig. 2 D and E). The number of counted cells is indicated.

Tauriello et al.

www.manaraa.com

Dvl1 DEP-C Interacts Directly with the Fz5 Discontinuous Binding Surface. To reveal what region of Dvl1-ΔDIX binds to the discontinuous binding surface on Fz, we generated additional His-tagged recombinant Dvl1 fragments (Fig. 4A) and studied their interaction with the Fz5 peptide library. In agreement with previous work (23), we confirmed binding of the Dvl PDZ domain (S201–P375) to the classic motif in the Fz5 C terminus. The PDZ domain, however, did not bind any iLoop3 sequence (Fig. 4B and Fig. S1A). We therefore interrogated a Dvl fragment comprising the DEP-C (R376–M695) for Fz5 binding. Strikingly, two DEP-C interaction modes with Fz5 peptides became apparent. In one prominent binding mode, the DEP-C fragment faithfully copied interaction with all three motifs as shown for Dvl1-ΔDIX (Figs. 1D and 4C). This DEP-C binding mode required the combined presence of either motif I or II with motif III, suggesting that the DEP-C domain mediates Dvl binding to the three-segmented binding surface on Fz5 (Fig. 4C and Fig. S1B). In the second binding mode, DEP-C interacts with a shifted membrane-proximal motif in the Fz C-terminal tail, comprising the classic Dvl interaction motif (Fig. 4D). This binding mode did not include the Fz5 iLoop3 motifs.

Next, we separately analyzed binding of the isolated DEP domain and the Dvl C terminus to the Fz5 peptide library to determine which part binds the individual motifs in the Fz5 interaction surface. The DEP domain preferentially bound motif III with a weak preference for peptides that include motif II but not motif I (Fig. 4E and Fig. S1C). Interestingly, the Dvl C-terminal fragment specifically bound Fz5 iLoop3 motifs I and II but entirely lacked affinity for motif III (Fig. 4F and Fig. S1D). These complementary binding patterns strongly argue for a model in which the DEP domain interacts with the Fz5 C-terminal tail and the Dvl C terminus mediates binding to the Fz5 iLoop3.

To compare and approximate the binding affinities of DEP and DEP-C for Fz5, we used a fluorescein-labeled peptide containing the Fz5 motifs II and III in fluorescence polarization (38). Binding curves indicate a 2- to 2.5-fold higher affinity of the DEP-C fragment for Fz5 peptide compared with the DEP domain, with an apparent K_d from two independent experiments of 6.5–12 µM for DEP-C vs. 22–30 µM for DEP (Fig. 4G). We conclude that the Dvl1 DEP domain is able to bind Fz5 directly but requires the C-terminal region to attain optimal binding affinity. Indeed, the isolated Dvl C terminus carries an intrinsic capacity to bind to the motif II-III Fz5 peptide with an estimated K_d of 13 µM (Fig. 4H).

Binding of Dvl DEP-C to Motifs I and II in Fz Is Critical for Wnt/β-Catenin Signaling in Cells. Our data indicate a key role for Dvl DEP-C in binding Fz. To examine the role of the DEP and DEP-C regions in Wnt/β-catenin signaling in cells, we generated a set of Flag-tagged Dvl1 fragments for expression in HEK293T cells (Fig. 5A). Ectopic expression of the DEP and DEP-C fragments, but not the PDZ domain, strongly inhibited Wnt3a-induced β-catenin–dependent transcription (28, 29) (Fig. 5B). These findings suggest that in contrast to the PDZ domain, the isolated DEP domain is sufficient to interfere with endogenous Fz-Dvl binding and signaling. Moreover, in contrast to full-length Dvl1, a Dvl1 variant lacking the DEP-C region failed to induce Wnt signaling on overexpression (39) and was not recruited to Fz5 (Fig. 5C and Fig. S2).

To substantiate these results, we determined the minimal required region of Dvl1 to bind Fz5 in cells. First, we confirmed that the Dvl1 DIX domain is dispensable for interaction with Fz5 (9, 27) (Fig. 5C and Fig. S2). The isolated Dvl1 PDZ domain, which binds the Fz C terminus with moderate affinity in vitro (23) (Fig. 4B), failed to bind Fz5 on coexpression (Fig. 5C and Fig. S2), as shown previously (29). In contrast, the Dvl1 DEP-C fragment robustly colocalized with Fz5, identical to full-length Dvl1 (Fig. 5C and Fig. S2). The Dvl1 DEP domain,
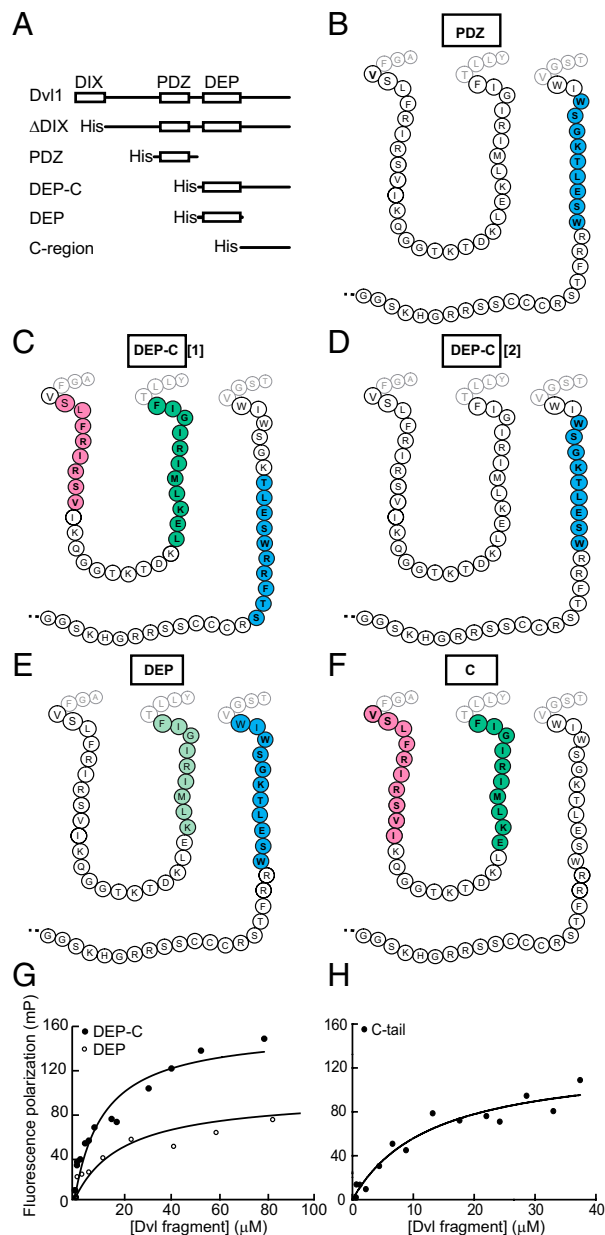
Fig. 4. Dvl1 DEP-C region binds the discontinuous binding surface in Fz5. (A) Domain structure of Dvl1 with three conserved domains (DIX, PDZ, and DEP), followed by a C-terminal region (C-region). His-tagged recombinant Dvl1 fragments that were generated are shown. (B–E) Fz5 binding motifs of indicated purified recombinant Dvl fragments. Details of best binding Fz peptides are described in Fig. S1. (B) Isolated PDZ (S201–P375) domain binds the Fz C-terminal tail, which comprises the classic PDZ binding sequence (motif III). (C) DEP-C region (R376–M695) binds the entire Fz discontinuous binding surface comprising motifs I, II, and III. (D) Alternative binding mode of DEP-C, involving the classic Fz C-terminal motif but not iLoop3. (E) DEP (S393–N503) domain without the C-region binds motif III in the Fz C-terminal tail and weakly to motif II. (F) Isolated C-region (L500–M695) binds motifs I and II in Fz5 iLoop3. (G) In vitro fluorescence polarization binding assay between a concentration range of recombinant DEP-C (filled) or DEP (open) and a cysteine-maleimide–linked fluorescein-labeled peptide (CKLMIR-IGIFGTLESWRRFTG, 100 nM) combining motifs II and III. The titration data are fitted with a binding saturation curve. One representative experiment of two is shown. (H) In vitro fluorescence polarization binding assay (as in G) using recombinant Dvl C-tail.

lacking its C-terminal extension, interacts with Fz5 in a less efficient manner (Fig. 5C and Fig. S2), confirming a role of the
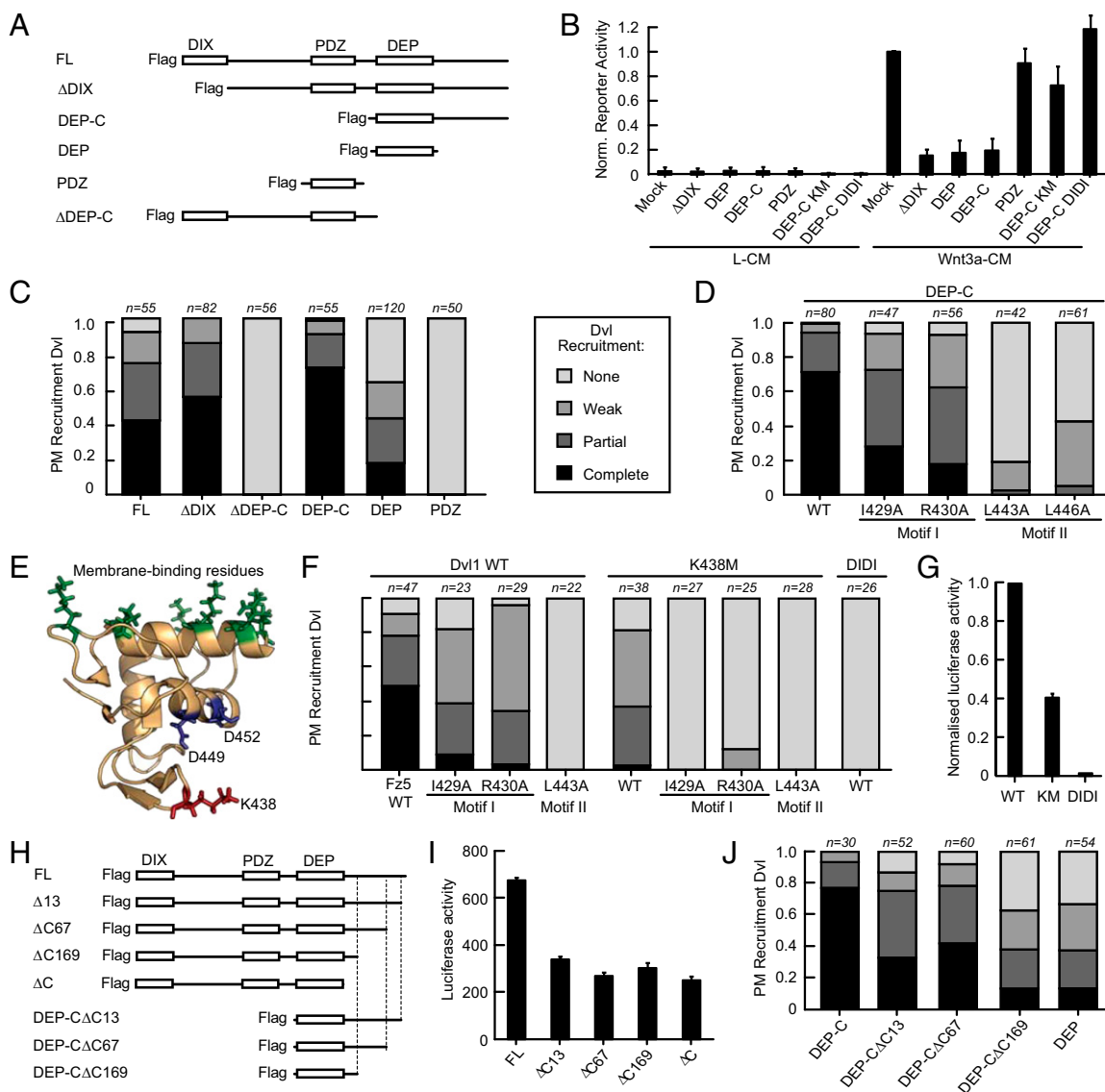
Fig. 5. Isolated DEP and DEP-C domains colocalize with Fz5 in cells and interfere with Wnt/β-catenin signaling. (*A*) Set of N-terminally Flag-tagged Dvl1 fragments. (*B*) HEK293T cells were transfected with indicated Dvl fragments and the TOPFlash /FOPFlash reporter constructs for 24 h and treated overnight with L-cell medium (L-CM) or Wnt3a-conditioned medium (Wnt3a-CM). Ectopic expression of ΔDIX, DEP-C, and DEP, but not mutated DEP or PDZ fragments, inhibits Wnt3a-induced β-catenin signaling. Data are represented as normalized averages of three individual experiments; error bars depict SDs. Mock, empty vector; KM, K438M; DIDI, D449I/D452I. (*C*) WT Fz5-mediated recruitment of Dvl1 constructs in HEK293T cells, analyzed by confocal immunofluorescence microscopy and quantified as in Fig. 2*E*. (*D*) Recruitment of Dvl1–DEP-C to Fz5 iLoop3 variants is partially and strongly impaired for motif I and motif II mutants, respectively. (*E*) DEP domain structure (28), indicating the membrane binding positively charged residues (green), as well as the K438 (red), D449 and D452 (blue) residues. (*F*) Recruitment of K438M and DIDI Dvl1 to mFz5 variants at the PM is strongly impaired. (*G*) DEP domain residues K438 and D449/D452 participate in Wnt/β-catenin signaling. Dvl variants were expressed in HEK293T cells, together with the TOPFlash luciferase reporter constructs, and analyzed for reporter activity after 24 h. (*H*) Set of Flag-tagged C-terminal truncations was generated in both full-length (FL) Dvl1 and the DEP-C fragment. (*I*) Most C-terminal region of Dvl1 significantly contributes to Dvl-mediated β-catenin activation, as analyzed by the TOPFlash reporter assay. (*J*) Extreme C-terminal Dvl1 region plays a role in Fz5-mediated PM recruitment of Dvl1. In addition, a second, more upstream region (spanning residues H526–S628) in the Dvl C terminus contributes to Fz-mediated PM recruitment. (*C*, *D*, *F*, and *J*) Number of counted cells per condition is indicated.

Dvl1 C terminus in Fz5 binding. DEP-C binding to Fz5 is either partially or dramatically impaired on mutation of motifs I and II, respectively (Fig. 5*D*). These results indicate that, as with full-length Dvl, either motif is required but not sufficient for efficient DEP-C recruitment, with a more prominent role of motif II.

Next, we asked how Fz function in cells correlates with the direct binding of Dvl DEP-C to Fz motifs I and II in vitro. To address this issue, we performed alanine-scanning mutagenesis on a 30-mer peptide library representing the full iLoop3 of Fz5.

Overall, alanine substitution of individual residues in motifs I and II, but not in the flanking sequence, diminished binding of DEP-C and ΔDIX-Dvl. This indicates that intact motifs I and II are required for optimal binding in vitro (Fig. S3*A*). Moreover, the levels of Dvl binding to individual mutant iLoop3 peptides significantly correlated with the signaling activity of the equivalent full-length Fz variants in cells (Fig. S3*B*; $r = 0.51$, $P = 0.007$). We conclude that Fz-mediated signaling relay to β-catenin critically depends on the direct interaction of Dvl DEP-C with iLoop3 motifs I and II.

Tauriello et al.

www.manaraa.com

We noted that within the 30-mer iLoop3 sequence, the I448A mutant behaved as a single outlier in this analysis. The I448A mutation diminished Dvl binding in vitro but, in the context of both the full-length Fz5 and XFz7 receptors, displayed robust Dvl recruitment and signaling in vivo (Figs. 2 *A* and *E* and 3 *C* and *E*, and Fig. S3*A*). We speculate that the reduction of Dvl binding by I448A may be compensated for by interactions through other regions or residues in full-length Fz5.

Identification of Critical Regions in the DEP-C Fragment for Fz Binding and Wnt/β-Catenin Signaling. Which residues at the surface of the DEP domain participate in Fz binding? Based on interactions of the DEP domain with lipid and protein partners at the PM (30–32), we reasoned that unoccupied surface-exposed DEP domain residues may mediate binding to Fz. A number of DEP domain variants, including the K438M mutation and the combined D449I and D452I mutations, were previously proposed to impair Fz-dependent PM recruitment (23, 29, 32) (Fig. 5*E*). Binding of Dvl1 K438M to WT Fz5 was strongly decreased, and the interaction was entirely lost in combination with Fz5 motif I/II mutants (Fig. 5*F*). Concurrently, the K438M Dvl1 mutant displays significantly decreased signaling activity (Fig. 5*G*). Mutation of D449/D452 (DIDI) fully abrogates both Fz5-mediated PM recruitment and signaling, preventing further analysis of the contribution of Fz motifs I and II (Fig. 5 *F* and *G*). Isolated Dvl1 DEP-C fragments with either of these mutations fail to inhibit Wnt3a-induced signal relay, confirming their inability to interact and interfere with the activity of endogenous Wnt signaling components (Fig. 5*B*). We conclude that Fz–DEP-C binding requires the cooperative use of Dvl DEP K438 and Fz motifs I and II at the binding interface to mediate PM recruitment of Dvl and Wnt/β-catenin signaling in cells.

To determine which regions in the Dvl1 C terminus are important for Fz association and Dvl signaling, we generated a number of progressive C-terminal truncations in both full-length Dvl1 and the Dvl1 DEP-C fragment (Fig. 5*H*). Loss of the extreme 13 amino acids (Dvl1ΔC13), which locate to a highly conserved region in all three Dvl isoforms, reduced the signaling capability of Dvl1 to the level of Dvl1ΔC. This indicates that the conserved C-terminal region contains important residues for Dvl signaling (Fig. 5*I*). Indeed, truncation of the terminal 13 amino acids from the DEP-C fragment resulted in reduced binding to Fz5 (Fig. 5*J*). Further truncation of the C-terminal region diminished the interaction with Fz5 even more, pointing to a second Fz binding region in the Dvl1 C terminus (Fig. 5*J*).

Discussion

Fz and Dvl act together in the control of Wnt-induced β-catenin–dependent and –independent pathways, but the underlying molecular mechanisms remain poorly understood (5, 40). A thorough understanding of the mechanism of Fz–Dvl complex formation is crucial to clarify how downstream signaling events are controlled. Moreover, Fz-Dvl interactions provide an attractive target for the design and development of drugs that interfere with Wnt signaling activation (24, 41–43). Although the Dvl PDZ domain was shown to bind an Fz C-terminal tail-derived peptide in vitro (9, 23), evidence for in vivo binding of the Dvl PDZ domain to Fz remains scarce. In addition, the affinity of this interaction is insufficient to explain the formation of a stable Fz–Dvl complex in cells, leading to the suggestion that additional intermolecular interactions are required (30, 32).

Here, we use a combinatorial peptide library that mimics the cytoplasmic surface of the Fz5 iLoop3 and C terminus to elucidate molecular recognition modes between Fz5 and Dvl1. We uncover a conserved binding mode in which Dvl interacts with a discontinuous binding site in Fz. Our results argue for cooperative binding of Dvl to the Fz C-terminal motif III and iLoop3 motifs I and II based on the following observations. First,

the strongest in vitro Dvl binding was observed for Fz peptides that combined either motif I or II with motif III. Second, mutations of single residues in either motif strongly impair Fz-mediated β-catenin–dependent signaling in cells and developing *Xenopus*, and abrogate the interaction with Dvl. These findings suggest that each of the motifs is required but not sufficient to mediate Fz-Dvl binding in cells. Furthermore, motif II appears more critical for Wnt/β-catenin signaling and complex formation with Dvl than motif I. These findings provide a mechanistic explanation for a couple of long-standing signaling-defective *fz* alleles in *Drosophila* (18, 44). Mutations in these *fz* alleles affect critical residues in the newly identified motif I or motif II, strongly suggesting that defective Dvl binding underlies its functional impairment in both Wnt/β-catenin and PCP pathways. Taken together, the Fz iLoop3 and C-terminal tail comprise a discontinuous Dvl binding site, which appears as a single binding surface when drawn on a 3D model of Fz as a GPCR-like protein (Fig. 6). The enhanced structural complexity of the three-segmented Fz motif compared with a single linear Dvl binding sequence entails possibilities for precise regulation of the interaction by allosterically induced conformational changes and/or posttranslational modification, as described for classic GPCRs (45).

Which domains of Dvl participate in binding the discontinuous Fz interface? We confirm binding of the Dvl1 PDZ domain to Fz5 C-terminal tail peptides that contain the classic KTxxxW Dvl binding motif (Fig. 4*B* and Fig. S1*A*), but we did not detect any interaction of PDZ with Fz5 iLoop3. Instead, we uncover that the Dvl1 DEP-C domain consistently binds all three motifs within the Fz5 discontinuous surface. Thus, the DEP-C domain fully copies the binding mode of the larger ΔDIX-Dvl1 protein, which also comprises the PDZ domain. In support of in vivo relevance of these findings, we demonstrate recruitment of the isolated DEP-C fragment, but not the PDZ domain, to Fz5 at the PM in cultured cells (Fig. 5*C* and Fig. S2). Of note, the yeast Sst2 DEP domain was previously shown to bind the GPCR family member Ste2, which is distantly related to Fz receptors, suggesting involvement of a highly conserved binding mode (46).

Next, we asked how the Dvl DEP-C domain docks onto the Fz receptor. Based on our combined in vitro peptide binding analysis and Fz interaction studies in cells, we propose a model in which the DEP domain mainly interacts with the Fz C-terminal tail (motif III), whereas the Dvl1 C terminus binds Fz iLoop3 (motifs I and II) (Fig. 6). Interestingly, the DEP-C fragment displayed an additional binding mode in which only the Fz C terminus (motif III) is occupied. Because this binding mode resembles the interaction of the isolated DEP domain with Fz, we consider it likely that the DEP-C domain does not use its
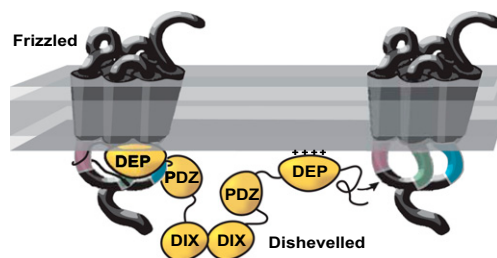
Fig. 6. Fz-Dvl interaction model. GPCR-like representation of Fz as a heptahelical TM protein. The discontinuous Dvl binding surface in the Fz iLoop3 and C-terminal tail is indicated. Dvl comprises three conserved, folded domains of which the PDZ, DEP domain, and extended C terminus are able to interact with the Fz interface. We propose that the DEP domain interacts with negatively charged lipid head groups to stabilize the Fz-Dvl interaction further. The DIX domain does not bind Fz and is free to multimerize and form receptor clusters.

C-terminal extension in this alternative orientation. Of note, a number of Fz family members, including Fz3 and Fz6, display loss of sequence conservation within the region of motif I. We speculate that weakening or alteration in Dvl binding to motif I in these Fzs may affect the orientation of Dvl in the bound state. Both Fz3 and Fz6 were previously linked to Wnt-induced β-catenin–independent PCP signaling (47). Thus, alternative Dvl binding modes may steer selective downstream signaling events.

Further probing of the Dvl interaction surface revealed that a number of surface-exposed residues (K438 and D449/D452) on the DEP domain as well as the last 13 residues of the C terminus are critical for functional interaction with Fz. Of note, based on secondary structure prediction, the entire Dvl C region is predicted to be intrinsically disordered, except for the last highly conserved 15–20 amino acids, which may fold and act as a functional terminal unit at the highly flexible Dvl C terminus.

How does the DEP domain accommodate different molecular interactions implicated in membrane recruitment? Recently, a positively charged stretch in the DEP domain was shown to interact directly with negatively charged lipids at the PM, suggesting a prominent role of lipid binding by the DEP domain in Fz-mediated signaling (30). Because membrane recruitment of DEP and DEP-C fragments codepends on the presence of Fz receptors (Fig. S2), we propose that the Dvl DEP-C domain may simultaneously bind lipids as well as the three motifs in the Fz receptor to stabilize the interaction (Fig. 6). Moreover, Fz intracellular loops 1 and 2 may contribute to Dvl binding as well. Taken together, we suspect that the affinity of DEP-C for Fz binding in vivo may be significantly increased through avidity effects of the local concentration of Dvl binding sites.

We conclude that the critical role of the Dvl1 DEP-C region in Wnt/β-catenin signaling is mediated through its direct interaction with a discontinuous binding surface on the Fz5 receptor. Our work suggests that Dvl employs multiple contact points with Fz and that each interaction is required for efficient downstream signaling to β-catenin. Whether binding events that involve the PDZ or DEP-C domain act cooperatively or sequentially awaits further investigation. We speculate that the DEP-C domain may be dominant over PDZ binding based on its expected higher affinity for Fz in vivo. Alternatively, simultaneous binding of both PDZ and DEP-C may allow a single Dvl molecule to form a complex with two Fzs.

We propose that the individual interactions may be subject to regulation by conformational changes and posttranslational modifications. Because Fz-Dvl signaling is implicated in at least two important Wnt pathways, detailed studies aimed at understanding how this interaction is induced and regulated by Wnt stimulation will help to explain how the Fz-Dvl functional unit manages to interpret upstream signals to disparate downstream pathways.

Methods

Cell Culture and Transfection. HEK293T cells and mouse L cells were cultured in RPMI or DMEM (Invitrogen), respectively, supplemented with 10% (vol/vol) FBS (Sigma), 100 units/mL penicillin, and 100 μg/mL streptomycin. L cells stably expressing Wnt3a have been described previously (39). Transfections were performed with FuGENE 6 (Roche) according to the manufacturer's protocol.

Constructs and Antibodies. V5-Fz5, Flag-Dvl1 variants, TOPFlash, and control FOPFlash luciferase reporter plasmids have been described previously (39). XWnt8 DNA and XFz7-myc were kind gifts of Randy Moon (University of Washington, Howard Hughes Medical Institute, Seattle, WA) and Herbert Steinbeisser (Heidelberg University Hospital, Institute of Human Genetics, Heidelberg, Germany), respectively. Alanine substitutions were generated by site-directed mutagenesis. Flag- or His-Dvl1 constructs were PCR-subcloned into pcDNA3 or a modified pET-24a(+) vector (Novagen), as described previously (48). For immunoblotting and immunofluorescence, mouse anti-

Flag (M2; Sigma), mouse anti-actin (C4; MP Biomedicals), mouse anti-V5 (Invitrogen), or rabbit anti-V5 (Sigma) was used.

TOPFlash Reporter Assays. HEK293T cells were seeded in 24-well plates and transfected with 30 ng of reporter construct TOPFlash or FOPFlash, 5 ng of thymidine kinase (TK)-Renilla, 50 ng of Dvl constructs, 35 ng of Fz constructs, and mock plasmid to a total of 250 ng per well. The assay was performed as described previously (39).

Confocal Microscopy. HEK293T cells were grown on glass coverslips in 24-well plates (coated with laminin). Cells were transfected and fixed after 24 h in 4% (mass/vol) paraformaldehyde or ice-cold methanol, treated with blocking buffer [2% (mass/vol) BSA, 0.01% saponin in PBS], and incubated with primary antibodies, followed by secondary antibodies conjugated to Alexa-488, Alexa-568, or Cy5. Cells were mounted in ProLong Gold (Invitrogen) and visualized using a Zeiss LSM510 confocal microscope.

Protein Purification. His-tagged Dvl fragments were expressed in Rosetta2 cells, induced at an OD_{600} of 0.6 with 0.5 mM isopropyl-β-D-thiogalactopyranoside for 6 h at 20 °C. Bacterial cell pellets were resuspended in buffer containing 50 mM Tris (pH 7.5, 8.0, or 9.0), 300 mM NaCl, 5% (vol/vol) glycerol, 5 mM imidazole, 25 μM PMSF, 1 μg/mL DNase, 1 μg/mL RNase, 2 μg/mL lysozyme, and a 0.1-mL^{-1} tablet of EDTA-free protease inhibitor mixture (Roche); homogenized by French Press; and purified by ÄKTA purification, using a HisTrap Ni-NTA column (GE Healthcare). Proteins were eluted with an imidazole gradient, buffer-exchanged in 20 mM Tris and 150 mM NaCl using HiTrap and PD-10 desalting columns (GE Healthcare), and concentrated with vivaspin 6 columns (Sartorius-stedim).

Peptide Library Generation and Screening. The linear and CLIPS peptides were synthesized using standard Fmoc chemistry and deprotected using trifluoric acid with scavengers. Constrained peptides were synthesized on chemical scaffolds using CLIPS technology through cysteine residues (37). The Cys side chains were coupled to CLIPS templates by reacting onto credit-card format polypropylene PEPSCAN cards (Pepscan Therapeutics BV; 455 peptide formats per card) with a 0.5-mM solution of CLIPS template 1,3,5-Tris (bromomethyl) benzene in ammonium bicarbonate [20 mM (pH 7.9)]/acetonitrile (1:1 vol/vol)]. The cards were gently shaken for 30–60 min. Finally, the cards were washed extensively and sonicated in disrupt buffer containing 1% SDS/0.1% β-mercaptoethanol in PBS (pH 7.2) at 70 °C for 30 min, followed by sonication in H_2O for another 45 min.

Protein binding was analyzed in a PEPSCAN-based ELISA (Pepscan Therapeutics BV). The 455-well cards containing the covalently linked peptides were incubated with 1 μg/mL protein in blocking solution [4% (vol/vol) horse serum, 5% (mass/vol) ovalbumin, 1% Tween in PBS]. After washing, the peptides were incubated with a monoclonal mouse anti-His tag antibody (1:1,000; Novagen) and, subsequently, after washing, with a peroxidase-conjugated rabbit–anti-mouse antibody (1:1,000; Southern Biotech). After washing, the peroxidase substrate 2,2'-azino-di-3-ethylbenzthiazoline sulfonate and 2 μL of 3% H_2O_2 were added. Color development was measured and quantified with a CCD and an image processing system (49). After background correction, these raw data were ranked and the top 5% (48 peptides) were analyzed.

Fluorescence Polarization (FP). CKLMIRIGIFGTLESWRRFTG peptide was synthesized using standard Fmoc chemistry and deprotected using trifluoric acid with scavengers. The Cys side chain was labeled with fluorescein-maleimide. Peptide and purified recombinant proteins were diluted in FP buffer [50 mM Tris (pH 7.5), 50 mM NaCl, 5 mM β-mercaptoethanol] to 100 nM and 100 μM, respectively. A protein dilution series to subnanomolar range was incubated with the peptide for 15–30 min. Fluorescence polarization of the labeled peptide was analyzed in a Spectramax M5 plate reader (Molecular Devices). Data from the different incubation times were averaged and plotted. Using Sigmaplot (Systat), a binding saturation curve [$Y = B_{max} \times X/(K_d + X)$] was fitted, with Y as the measured FP value (F∥ − F∞)/(F∥ + F∞), B_{max} as the maximum value, and X as the Dvl fragment concentration. From this formula, the equilibrium constant, K_d, was derived as the protein concentration at one-half saturation.

Xenopus Embryo Axis Duplication and Dvl Recruitment Assays. Mature eggs were obtained by injecting females with 500 units of human chorion gonadotropin (Sigma). One hour after in vitro fertilization, the jelly coat was removed by treating the embryos with 2% (mass/vol) cysteine hydrochloride in 0.1× modified Barth's solution (MBSH) at pH 8.2 [1× MBSH: 10 mM Hepes,

88 mM NaCl, 1 mM KCl, 0.33 mM $Ca(NO_3)_2$, 0.41 mM $CaCl_2$, 0.82 mM $MgSO_4$, 2.4 mM $NaHCO_3$ (pH 7.4)]. Embryos were staged according to the method of Nieuwkoop and Faber (50). Capped mRNAs were transcribed from linearized DNA templates with a mMessage mMachine kit (Ambion).

For axis duplication assays, embryos were injected at the four-cell stage in the marginal zone of both ventral blastomeres with 0.1 pg of XWnt8 RNA plus 400 pg of XFz7-myc RNAs in a volume of 8 nL and kept in 0.1× MBSH at 16 °C until they had reached stage 21–22. For Dvl recruitment, embryos were injected at the two-cell stage in the animal pole of both cells with 200 pg of XDvl2-GFP RNA and 200 pg of XFz7-myc RNAs and kept in 0.1× MBSH at 16 °C until they reached stage 10. Embryos were fixed for 1 h in 4% (mass/mass) formaldehyde/1× MEM [100 mM 3-(N-morpholino)propanesulfonic acid (Mops) (pH 7.4), 2 mM EGTA, 1 mM $MgSO_4$] at room temperature and for an additional 4 h in DENT's (80% methanol, 20% DMSO) at −20 °C. After

rehydration, the animal caps were cut and blocked in 20% (vol/vol) horse serum for 1 h. Animal cap explants were stained with anti-GFP (Abcam) and an Alexa-488–conjugated secondary antibody, and nuclei were counterstained with Hoechst dye. Animal cap explants were mounted in Mowiol (Roth) and analyzed with a Zeiss Axio Imager D1/Z1.

1. Logan CY, Nusse R (2004) The Wnt signaling pathway in development and disease. *Annu Rev Cell Dev Biol* 20:781–810.
2. Clevers H (2006) Wnt/beta-catenin signaling in development and disease. *Cell* 127:469–480.
3. Reya T, Clevers H (2005) Wnt signalling in stem cells and cancer. *Nature* 434:843–850.
4. MacDonald BT, Tamai K, He X (2009) Wnt/beta-catenin signaling: Components, mechanisms, and diseases. *Dev Cell* 17:9–26.
5. Seifert JR, Mlodzik M (2007) Frizzled/PCP signalling: A conserved mechanism regulating cell polarity and directed motility. *Nat Rev Genet* 8:126–138.
6. van Amerongen R, Mikels A, Nusse R (2008) Alternative wnt signaling is initiated by distinct receptors. *Sci Signal* 1:re9.
7. Yang-Snyder J, Miller JR, Brown JD, Lai CJ, Moon RT (1996) A frizzled homolog functions in a vertebrate Wnt signaling pathway. *Curr Biol* 6:1302–1306.
8. Rothbächer U, et al. (2000) Dishevelled phosphorylation, subcellular localization and multimerization regulate its role in early embryogenesis. *EMBO J* 19:1010–1022.
9. Umbhauer M, et al. (2000) The C-terminal cytoplasmic Lys-thr-X-X-X-Trp motif in frizzled receptors mediates Wnt/beta-catenin signalling. *EMBO J* 19:4944–4954.
10. Sabharanjak S, Sharma P, Parton RG, Mayor S (2002) GPI-anchored proteins are delivered to recycling endosomes via a distinct cdc42-regulated, clathrin-independent pinocytic pathway. *Dev Cell* 2:411–423.
11. Bhanot P, et al. (1996) A new member of the frizzled family from Drosophila functions as a Wingless receptor. *Nature* 382:225–230.
12. Wang HY, Liu T, Malbon CC (2006) Structure-function analysis of Frizzleds. *Cell Signal* 18:934–941.
13. Schulte G, Bryja V (2007) The Frizzled family of unconventional G-protein-coupled receptors. *Trends Pharmacol Sci* 28:518–525.
14. Wu J, Klein TJ, Mlodzik M (2004) Subcellular localization of frizzled receptors, mediated by their cytoplasmic tails, regulates signaling pathway specificity. *PLoS Biol* 2:E158.
15. Djiane A, Yogev S, Mlodzik M (2005) The apical determinants aPKC and dPatj regulate Frizzled-dependent planar cell polarity in the Drosophila eye. *Cell* 121:621–631.
16. Cong F, Schweizer L, Varmus H (2004) Wnt signals across the plasma membrane to activate the beta-catenin pathway by forming oligomers containing its receptors, Frizzled and LRP. *Development* 131:5103–5115.
17. Wu J, Jenny A, Mirkovic I, Mlodzik M (2008) Frizzled-Dishevelled signaling specificity outcome can be modulated by Diego in Drosophila. *Mech Dev* 125:30–42.
18. Povelones M, Howes R, Fish M, Nusse R (2005) Genetic evidence that Drosophila frizzled controls planar cell polarity and Armadillo signaling by a common mechanism. *Genetics* 171:1643–1654.
19. Schweizer L, Varmus H (2003) Wnt/Wingless signaling through beta-catenin requires the function of both LRP/Arrow and frizzled classes of receptors. *BMC Cell Biol* 4:4.
20. Bilic J, et al. (2007) Wnt induces LRP6 signalosomes and promotes dishevelled-dependent LRP6 phosphorylation. *Science* 316:1619–1622.
21. Schwarz-Romond T, et al. (2007) The DIX domain of Dishevelled confers Wnt signaling by dynamic polymerization. *Nat Struct Mol Biol* 14:484–492.
22. Kishida S, et al. (1999) DIX domains of Dvl and axin are necessary for protein interactions and their ability to regulate beta-catenin stability. *Mol Cell Biol* 19:4414–4422.
23. Wong H-C, et al. (2003) Direct binding of the PDZ domain of Dishevelled to a conserved internal sequence in the C-terminal region of Frizzled. *Mol Cell* 12:1251–1260.
24. Zhang Y, et al. (2009) Inhibition of Wnt signaling by Dishevelled PDZ peptides. *Nat Chem Biol* 5:217–219.
25. Gao C, Chen Y-G (2010) Dishevelled: The hub of Wnt signaling. *Cell Signal* 22:717–727.
26. Lee HJ, et al. (2010) Identification of transmembrane protein 88 (TMEM88) as a dishevelled-binding protein. *J Biol Chem* 285:41549–41556.
27. Axelrod JD, Miller JR, Shulman JM, Moon RT, Perrimon N (1998) Differential recruitment of Dishevelled provides signaling specificity in the planar cell polarity and Wingless signaling pathways. *Genes Dev* 12:2610–2622.
28. Wong HC, et al. (2000) Structural basis of the recognition of the dishevelled DEP domain in the Wnt signaling pathway. *Nat Struct Biol* 7:1178–1184.
29. Pan WJ, et al. (2004) Characterization of function of three domains in dishevelled-1: DEP domain is responsible for membrane translocation of dishevelled-1. *Cell Res* 14:324–330.
30. Simons M, et al. (2009) Electrochemical cues regulate assembly of the Frizzled/Dishevelled complex at the plasma membrane during planar epithelial polarization. *Nat Cell Biol* 11:286–294.
31. Yu A, et al. (2007) Association of Dishevelled with the clathrin AP-2 adaptor is required for Frizzled endocytosis and planar cell polarity signaling. *Dev Cell* 12:129–141.
32. Yu A, Xing Y, Harrison SC, Kirchhausen T (2010) Structural analysis of the interaction between Dishevelled2 and clathrin AP-2 adaptor, a critical step in noncanonical Wnt signaling. *Structure* 18:1311–1320.
33. Boutros M, Paricio N, Strutt DI, Mlodzik M (1998) Dishevelled activates JNK and discriminates between JNK pathways in planar polarity and wingless signaling. *Cell* 94:109–118.
34. Li L, et al. (1999) Dishevelled proteins lead to two signaling pathways. Regulation of LEF-1 and c-Jun N-terminal kinase in mammalian cells. *J Biol Chem* 274:129–134.
35. Moriguchi T, et al. (1999) Distinct domains of mouse dishevelled are responsible for the c-Jun N-terminal kinase/stress-activated protein kinase activation and the axis formation in vertebrates. *J Biol Chem* 274:30957–30962.
36. Penton A, Wodarz A, Nusse R (2002) A mutational analysis of dishevelled in Drosophila defines novel domains in the dishevelled protein as well as novel suppressing alleles of axin. *Genetics* 161:747–762.
37. Timmerman P, Puijk WC, Meloen RH (2007) Functional reconstruction and synthetic mimicry of a conformational epitope using CLIPS technology. *J Mol Recognit* 20:283–299.
38. Jameson DM, Ross JA (2010) Fluorescence polarization/anisotropy in diagnostics and imaging. *Chem Rev* 110:2685–2708.
39. Tauriello DVF, et al. (2010) Loss of the tumor suppressor CYLD enhances Wnt/beta-catenin signaling through K63-linked ubiquitination of Dvl. *Mol Cell* 37:607–619.
40. Veeman MT, Axelrod JD, Moon RT (2003) A second canon. Functions and mechanisms of beta-catenin-independent Wnt signaling. *Dev Cell* 5:367–377.
41. Shan J, Shi D-L, Wang J, Zheng J (2005) Identification of a specific inhibitor of the dishevelled PDZ domain. *Biochemistry* 44:15495–15503.
42. Fujii N, et al. (2007) An antagonist of dishevelled protein-protein interaction suppresses beta-catenin-dependent tumor cell growth. *Cancer Res* 67:573–579.
43. Mahindroo N, Punchihewa C, Bail AM, Fujii N (2008) Indole-2-amide based biochemical antagonist of Dishevelled PDZ domain interaction down-regulates Dishevelled-driven Tcf transcriptional activity. *Bioorg Med Chem Lett* 18:946–949.
44. Jones KH, Liu J, Adler PN (1996) Molecular analysis of EMS-induced frizzled mutations in Drosophila melanogaster. *Genetics* 142:205–215.
45. Christopoulos A, Kenakin T (2002) G protein-coupled receptor allosterism and complexing. *Pharmacol Rev* 54:323–374.
46. Ballon DR, et al. (2006) DEP-domain-mediated regulation of GPCR signaling responses. *Cell* 126:1079–1093.
47. Wang Y, Guo N, Nathans J (2006) The role of Frizzled3 and Frizzled6 in neural tube closure and in the planar polarity of inner-ear sensory hair cells. *J Neurosci* 26:2147–2156.
48. Noutsou M, et al. (2011) Critical scaffolding regions of the tumor suppressor Axin1 are natively unfolded. *J Mol Biol* 405:773–786.
49. Slootstra JW, Puijk WC, Ligtvoet GJ, Langeveld JP, Meloen RH (1996) Structural aspects of antibody-antigen interaction revealed through small random peptide libraries. *Mol Divers* 1:87–96.
50. Nieuwkoop PD, Faber J (1994) *Normal Table of Xenopus laevis (Daudin)* (Garland, New York).